Prediction of thermal coagulation by AC inductive heating of $Mg_{1-x}Ca_xFe_2O_4$ ferrite powder

S. NOMURA*, S. MUKASA, T. MIYOSHI, N. OKABE
Department of Mechanical Engineering, Faculty of Engineering, Ehime University, 3, Bunkyo-cho, Matsuyama 790-8577, Japan
E-mail: nomu@eng.ehime-u.ac.jp

T. MAEHARA
Department of Physics, Faculty of Science, Ehime University, 2-5, Bunkyo-cho, Matsuyama 790-8577, Japan

H. AONO
Department of Materials Science and Engineering, Faculty of Engineering, Ehime University, 3, Bunkyo-cho, Matsuyama 790-8577, Japan

H. KIKKAWA, K. SATOU, S. YUMI, Y. WATANABE
The 2nd Department of Surgery, Ehime University, Shitsukawa, Toon, Ehime 791-0295, Japan

Published online: 28 March 2006

The purpose of this study is to investigate the thermal characteristics of $Mg_{1-X}Ca_X Fe_2O_4$ ferrite powder by applying AC magnetic field and to predict the effect of thermal coagulation in vivo. We found that heating characteristics of the ferrite powder became greater as the frequency through the 400 kHz to 700 kHz range. The highest heat generation was attained using 7–15 nm ferrite powder. We also carried out a heat transfer simulation in which we were able to demonstrate that this material has sufficient heat generating characteristics to thermally coagulate a tumor cell and that it is possible to predict the range of the coagulation from the present simulation.

1. Introduction

Hyperthermia is an alternative to the conventional surgical, chemical therapy and radiation therapies for cancer [1–4]. Hyperthermia takes advantage of the lower resistance to heat that a cancer cell has in comparison to a normal cell. In our investigation we examine a local thermal therapy that entails introducing a metallic or ferrite powder into tumor cells and then applying an external alternating magnetic field to selectively heat only the tumor cells to a temperature of 50–60°C, thereby inducing the total necrosis of the tumor [5–7].

Up until this investigation, we had been able to demonstrate that sufficient temperature for the necrosis of the tumor could be attained using Mg ferrite ($MgFe_2O_4$) with a particle size of 2–10 μm. The heat generation of $MgFe_2O_4$ was attributed to the large hysteresis loss in the magnetic properties. However, as the particle size was reduced, the nano order came into effect and the heating characteristics dropped, which required that a longer time in comparison with micro order particles was needed to achieve the desired temperature. [8]. Moreover, losses occurring in ferromagnetic particles may be differentiated in particle size or amplitude and frequency [9, 10].

In this study, we propose the use of a nano-size ferrite powder that contains calcium as a medium with good biocompatibility. Exchanging Ca in the cubic crystal structure of $MgFe_2O_4$ causes a deformation of the crystal cubic crystal structure from which we expect a dramatic increasing of the heating characteristics [7].

First, the inductive heating by alternating magnetic field was carried out using $Mg_{1-x}Ca_xFe_2O_4$ powder in which Mg^{2+} sites in cubic $MgFe_2O_4$ are substituted with Ca^{2+}. Second, based on the heat generation in this experiment the heat coagulation of a tumor is predicted by using a heat transfer simulation.

*Author to whom all correspondence should be addressed.
0022-2461
DOI: 10.1007/s10853-006-6749-7

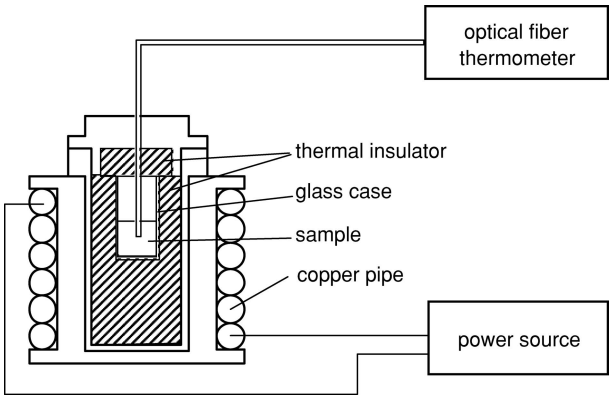

Figure 1. Experimental apparatus.

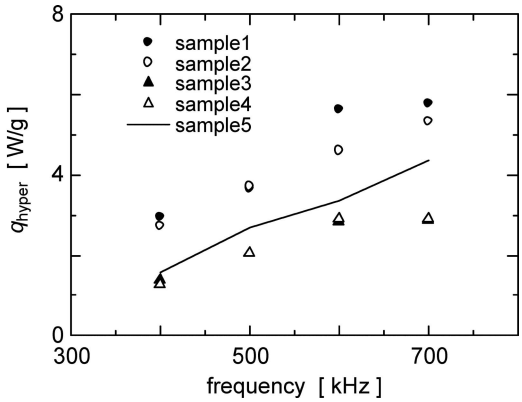

Figure 2. Heat generation of ferrite powder.

2. Experiment apparatus and methods

The apparatus used in the experiment is shown in Fig. 1. A 6-mm-diameter copper pipe is wrapped around the circumference of a polypropylene cylinder having an inner diameter of 48 mm and a height of 35 mm. This is used as the wave-guide for introducing the high-frequency waves. Coolant flows through the pipe to prevent a rise in its temperature. The test material is placed inside a heat-resistant glass case (Pyrex® grass), which is positioned in the center section of the coil. The glass case is insulated with a liquid hard polyurethane insulating material with thermal conductivity 0.03–0.04 W/(m · K). We were then able to investigate the characteristics of the rise in temperature as the high-frequency waves were applied. The temperature of the internal section of the test material was measured by an optical fiber thermometer. Details of the $Mg_{1-x}Ca_xFe_2O_4$ material used in this experiment are shown in Table I.

The ferrite powders were created with different firing temperatures in order to examine the affects of the different magnesium and calcium powder sizes. In addition, commercially available Mg ferrite powder $MgFe_2O_4$ (99.9%, Kojundo Chemical Lab. Co., Ltd.) was used to provide a comparison of the heat characteristics in this experiment.

The experiment was conducted by pouring 2 ml of water into the glass case and then dispersing 1 g of the test material in that water. An alternating magnetic field was then applied that had a frequency range between 400 and 700 kHz and a magnetic-field strength of 4 kA/m. The strength is usually adopted when experimenting on animals. The heat generation under these conditions was then observed.

TABLE I. Ferrite powders. Here, sample 5 obtained from commercial source, which did not provide the baking temperature

	Ferrite powder	Size	Baking temp
Sample 1	$Mg_{0.5}Ca_{0.5}Fe_2O_4$	7–15 nm	300°C
Sample 2	$Mg_{0.5}Ca_{0.5}Fe_2O_4$	130 nm	800°C
Sample 3	$Mg_{0.3}Ca_{0.7}Fe_2O_4$	5–20 nm	300°C
Sample 4	$Mg_{0.3}Ca_{0.7}Fe_2O_4$	130 nm	800°C
Sample 5	$MgFe_2O_4$	2–10 μm	unknown

3. Results of experiment and observation

The relationship between heat generation per unit mass of ferrite powder (q_{hyper}) and frequency is shown in Fig. 2. The heat generation from each of the test materials was calculated based on the relative rise in the water temperature at that time, based on the assumption that all of the heat generated from ferrite powders was used for raising the temperature of the water [6].

Regardless of the material, the amount of heat generated increased as the frequency increased. There was a great dependence on frequency even when the magnetic-field strength was stable. The $Mg_{1-x}Ca_xFe_2O_4$ showed heating characteristics equal to or superior than the Mg ferrite in spite of the nano-order particles. The particle diameter of 7–15 nm shown in Sample 1 yielded the highest heat generation with 5.8 W/g. This amount of heat generation was approximately 1.3 times greater than the maximum heat generation of 4.4 W/g attained with $MgFe_2O_4$ in Sample 5.

The dominant loss mechanism is still unclear [10]. The small particle size shown in Sample 1 was found to have the largest loss. When introducing powders into the body, there is the danger that the powders that do not adhere to the cancerous tissue may go on to block the capillaries in healthy tissue. Since the $Mg_{1-x}Ca_xFe_2O_4$ has a smaller size and offers higher heat characteristics than the $MgFe_2O_4$, it is extremely well suited as the powder material to be used as the coagulating material.

4. Numerical analysis

4.1. Analytical model

We solve the three dimensional unsteady state heat conduction equation [11, 12] as shown in Eq. (1) that takes into account the amount of heat generation by ferrite powder, the heat due to the regeneration of the tissue and the cooling effect of blood flow in an attempt to analyze heat conduction as it relates to local thermotherapy.

$$\rho_{body} C_{pbody} \frac{\partial T(x, y, z, t)}{\partial t} = \lambda_{body} \nabla^2 T(x, y, z, t) + Q_{hyper} + Q_{body} - w_{blood} C_{pblood} \left(T(x, y, z, t) - T_{body} \right) \quad (1)$$

The left section of the equation has the unsteady term, the right section has the heat conduction, the heat generation of the ferrite powder, the heat generation due to the fundamental regeneration of the tissue and the final term shows the cooling from blood flow. The following are used in this analysis: density of body tissue (λ_{body}) is 1000 kg/m^3 specific heat ($C_{p\ body}$) is 3852 J/(kg·K), thermal conductivity (λ_{body}) is 0.64 W/(m·K), and 4185 J/(kg·K) is used as the specific heat of the blood ($C_{p\ blood}$). In addition, a blood flow volume (w_{blood}) of 12 kg/(m^3·s) and the heat caused by metabolism (Q_{body}) of 1000 W/m^3 are used for the tissue before the onset of coagulation. These physical properties used in the analysis are taken from refs. 13 and 14. It is determined that coagulation of the tissue occurred when the temperature of the tissue is exposed to temperatures of 42.5°C or more for 30 s, so after that point, the analysis is made using zero as the heat generated from tissue. This reference temperature is almost equal to the temperature used in the majority of hyperthermia experiments. This study is not concerned with determining apoptosis or necrosis as the dominant mechanism of coagulation. Here, we propose the prediction of coagulation area in vivo by using numerical simulation.

A growth with a central size of 30 × 30 × 30 mm is used in the analysis and it is assumed the ferrite powder that serves as the heating source is evenly distributed within a specified symmetrically spherical area from the center. During actual treatment, a ferrite fluid in which minute ferrite powders have been dispersed would be introduced to the body through a catheter or other means. According to calculations, the introduced ferrite powder of 0.05–0.6 g would be distributed within a spherical area of a radius ranging from 3 mm to 15 mm, and the density of the distributed ferrite powder is fluctuated randomly within ±20%.

4.2. Cooling effect of blood flow

The upper graph of Fig. 3 shows heat distribution from the center and the heat flux due to thermal conductance at 1800 s after the application of AC magnetic wave was started. The lower graph shows the each of the values for the heat and cooling terms from the second term to the forth term of Eq. (1). We used the value (5.8 W/g) for the 700 kHz application as the heat generation of the ferrite power because it is the maximum value obtained in the experiment with sample 1, as shown in Fig. 2. The weight of the powder (m_{fer}) was 0.2 g and the distribution radius (r_{dist}) was 8 mm. At this time, the mass ratio of ferrite powder to tumor tissue (an 8 mm radius sphere) was approximately 10%. The heat density of the ferrite powder in the area of the coagulation was 5 × 10^5 W/m^3, which corresponds to approximately 500 times metabolic heat. The radius of the coagulation tissue is 8 mm, equal to the distribution radius. Since the blood flow in the coagulation area is stopped, all of the heat generated by the ferrite powder is transferred to the outer side of the tumor by thermal conduction so the area near the outer surface

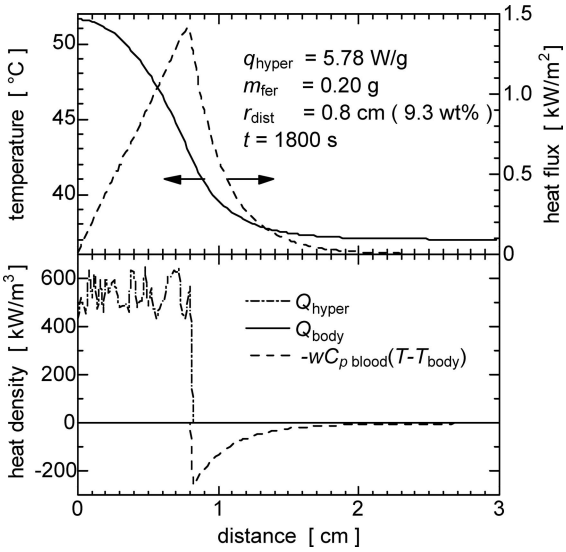

Figure 3. Profiles of temperature, heat flux, and heat generation per unit volume. Here, the mass ratio of the ferrite powder to the tumor is 9.3% when r_{dist} = 0.8 cm and m_{fer} = 0.2 g. It is denoted that Q_{body} = 1 kW/m^3 in over 0.8 cm although it seems to be zero.

of the coagulation is rapidly cooled by blood flow. The cooling effect of the blood flow extends to approximately 2 cm radius.

4.3. Prediction of the coagulation area

Fig. 4 shows the growth of the coagulation area when the AC magnetic waves are applied. During the initial period of approximately 200 s, the coagulation area grows quickly but after a while a balance is reached between the amount of heat and the amount of cooling due to surrounding blood flow, and tends to become saturated. In addition, while the growth process will differ slightly according to differences in the distribution of the ferrite powder, when the steady state is reached after 500 s, the radius of the coagulation tissue will be even regardless of the state of the distribution. However, when the radius

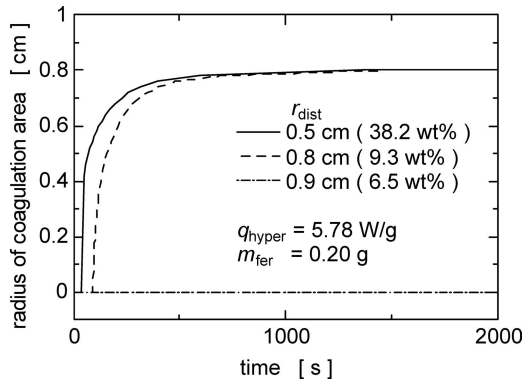

Figure 4. Prediction of coagulation area by inductive heating. The mass ratio of the ferrite powder of 0.2 g to the tumor is 6.5% when r_{dist} = 0.9 cm, 9.3% when r_{dist} = 0.8 cm and 38.2% when r_{dist} = 0.5 cm.

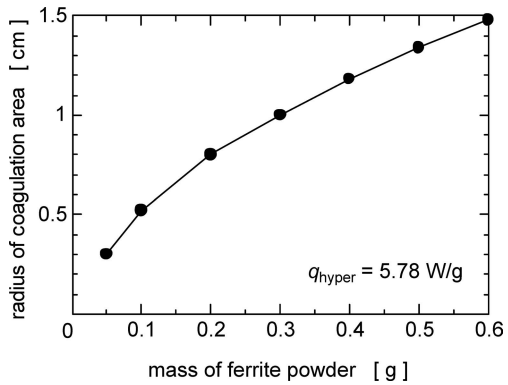

Figure 5. Effect of mass of ferrite powder in coagulation area. Here, the distribution radius of the ferrite powder is equal to or smaller than the radius of the coagulation area, for example $r_{dist} = 0.3$ cm when $m_{fer} = 0.05$ g, $r_{dist} = 0.5$ cm when $m_{fer} = 0.1$ g, $r_{dist} = 0.8$ cm when $m_{fer} = 0.2$ g, $r_{dist} = 1.0$ cm when $m_{fer} = 0.3$ g, $r_{dist} = 1.1$ cm when $m_{fer} = 0.4$ g, $r_{dist} = 1.3$ cm when $m_{fer} = 0.5$ g and $r_{dist} = 1.4$ cm when $m_{fer} = 0.6$ g, where m_{fer} is the mass of ferrite powder.

of the distribution exceeded 0.9 cm, coagulation did not occur because of the insufficient heating.

Fig. 5 shows the radius of the coagulative tissue in the steady state when the amount of the ferrite powder is changed. To make the coagulation area shown in Fig. 5 grow, the ferrite powder must be distributed to an area equal to or smaller than the coagulation area shown in Fig. 5. If the distribution area is larger than the area shown in Fig. 5, the coagulation area may grow to an area smaller than that shown in Fig. 5 or may not grow at all because of insufficient heating. The average size of the common tumor is approximately 15 mm. Based on this, the amount of ferrite powder introduced in relation to the size of the tumor in the preliminary diagnosis can be adjusted to enable coagulation of only the tumor cells. In addition, the time for the treatment is approximately 500 s.

5. Conclusions

An induction heat experiment was conducted by applying an AC magnetic field with a frequency of 400–700 kHz to $Mg_{1-x}Ca_xFe_2O_4$ powder having a particle diameter of 7–130 nm. The amount of heat generation by the ferrite powder increases proportionately with the increase in the applied frequency. When $Mg_{0.5}Ca_{0.5}Fe_2O_4$ powder with a particle diameter of 7–15 nm is used, a maximum of 5.8 W/g can be attained. Furthermore, it is possible to predict the tumor temperature and coagulation area by a heat transfer simulation that takes the heat generation of ferrite powder, the metabolism heat and the cooling effect of blood flow into account.

References

1. A. JORDAN, P. WUST, H. FÄHKING, W. JOHIN, A. HINZ and R. FELIX, *Int. J. Hypertheamia* **9** (1993) 51.
2. M. MITSUMORI, M. HIRAOKA, T. SHIBATA, Y. OKUNO, S. MASUNAGA, M. KOISHI, K. OKAJIMA, Y. NAGATA, Y. NISHIMURA, M. ABE, K. OHURA, M. HASEGAWA, H. NAGAE and Y. EBISAWA, *Int. J. Hypertermia* **10** (1994) 785.
3. C. GUIOT, R. CAVALLI, P.GAGLIOTI, D. DANELON, C. MUSACCHIO, M. TROTTA and T. TODROS, *Ultrasonics* **42** (2004) 927.
4. R. KAATEEA, P. NOWAKB, J. ZEEC, J. BREED, B. KANISA, H. CREZEED, P. LEVENDAGB and A. VISSER, *Radio. Oncol.* **59** (2001) 227.
5. T. MAEHARA, K. KONICHI, T. KAMIMORI, H. AONO, T. NAOHARA, H KIKKAWA, Y. WATANABE and K. KAWACHI, *Jpn. J. Appl. Phys.* **41** (2002) 1620.
6. T. MAEHARA, K. KONISHI, T. KAMIMORI, H. AONO, H. HIRAZAWA, T. NAOHARA, S. NOMURA, H. KIKKAWA, Y. WATANABE and K. KAWACHI, *J. Mater. Sci.* **40** (2005) 135.
7. H. AONO, H. HIRAZAWA, T. OCHI, T. NAOHARA, K. MORI, Y. HATTORI, T. MAEHARA, H. KIKKAWA and Y. WATANABE, *Chem. Lett.* **34** (2005) 482.
8. S. NOMURA, S. MUKASA, H.YAMASAKI, T. MAEHARA, H. AONO, H. KIKKAWA, K. SATOU, S. YUMI and Y. WATANABE, *Heat Trans. Eng.* (2005) submitted.
9. R. HERGT, R. HIERGEIST, I. HILGER, W.A. KAISER, Y. LAPATNIKOV, S. MARGEL and U. RICHTER, *J. Magn. Magn. Mater.* **270** (2004) 345.
10. A. JORDAN, R. SCHOLZ, P. WUST, H. SCHIRRA, T. SCHIESTEL, H. SCHMIDT and R. FELIX, *J. Magn. Magn. Mater.* **194** (1999) 185.
11. C. THIEBAUT and D. LEMONNIER, *Int. J. Therm. Sci.* **41** (2002) 500.
12. R.DUA and S. CHAKRABOTRY, *Comp. Bio. Med.* **35** (2005) 447.
13. M. SEEBASS, R. BECK, J. GELLERMANN, J. NADOBNY and P. WUST, *ZIB-Report* **00–28** (2000, Oct) 10.
14. A. Y. MATLOUBIEH, R. B. ROEMER, and T. C. CETAS, *IEEE Trans. BME.* **31** (1984) 227–234.

Received 20 May
and accepted 29 August 2005